J Cardiovasc Imaging. 2020 Apr;28(2):94-105
https://doi.org/10.4250/jcvi.2019.0087
pISSN 2586-7210·eISSN 2586-7296

Journal of Cardiovascular Imaging JCVI

Original Article

Check for updates

Diagnostic Value of Lesion-specific Measurement of Myocardial Blood Flow Using Hybrid PET/CT

Sang-Geon Cho, MD, PhD[1], Hyeon Sik Kim, PhD[2], Jae Yeong Cho, MD, PhD[3], Ju Han Kim, MD, PhD[3], and Hee-Seung Bom, MD, PhD[4]

[1]Department of Nuclear Medicine, Chonnam National University Hospital, Gwangju, Korea
[2]Medical Photonics Research Center, Korea Photonics Technology Institute, Gwangju, Korea
[3]Department of Cardiovascular Medicine, Chonnam National University Hospital, Gwangju, Korea
[4]Department of Nuclear Medicine, Chonnam National University Hwasun Hospital, Jeollanam-do, Korea

OPEN ACCESS

Received: Sep 6, 2019
Revised: Oct 22, 2019
Accepted: Nov 27, 2019

Address for Correspondence:
Hee-Seung Bom, MD, PhD
Department of Nuclear Medicine, Chonnam National University Hwasun Hospital, 322 Seoyang-ro, Hwasun-eup, Hwasun-gun, Jeollanam-do 58128, Korea.
E-mail: hsbom@jnu.ac.kr

ORCID iDs
Sang-Geon Cho
https://orcid.org/0000-0002-1373-1887
Hyeon Sik Kim
https://orcid.org/0000-0001-9199-022X
Jae Yeong Cho
https://orcid.org/0000-0002-9393-2821
Ju Han Kim
https://orcid.org/0000-0002-3186-0770
Hee-Seung Bom
https://orcid.org/0000-0002-5570-7375

Conflict of Interest
The authors have no financial conflicts of interest.

ABSTRACT

BACKGROUND: We evaluated whether lesion-specific measurement of myocardial blood flow (MBF) and flow reserve (MFR) by hybrid imaging of myocardial perfusion positron emission tomography (PET) and coronary computed tomography (CT) can provide additional diagnostic value.
METHODS: Forty-three patients with stable angina underwent N-13 ammonia PET and coronary CT before invasive coronary angiography (CAG). The lesion-specific MBF was calculated from the average MBF of the myocardial segments downstream of a coronary stenosis using hybrid PET/CT images. The hyperemic MBF, resting MBF, and MFR were measured for the left anterior descending artery (LAD) using conventional and lesion-specific methods. The diagnostic accuracy was compared between the two methods for significant LAD stenoses (≥ 70% reference diameter on CAG).
RESULTS: There were 19 significant LAD stenoses. The sensitivity, specificity, negative predictive value, positive predictive value, and accuracy were 71%, 68%, 74%, 65%, and 70% for conventional hyperemic MBF (optimal cutoff = 2.15 mL/min/g), 79%, 63%, 74%, 65%, and 70% for conventional MFR (optimal cutoff = 1.82), 83%, 74%, 80%, 78%, and 80% for lesion-specific hyperemic MBF (optimal cutoff = 1.75 mL/min/g), and 79%, 79%, 83%, 75%, and 79% for lesion-specific MFR (optimal cutoff = 1.86), respectively. The lesion-specific measurement was more accurate and had a better linear correlation with anatomical stenosis severity for both hyperemic MBF and MFR.
CONCLUSIONS: Lesion-specific measurement using hybrid PET/CT imaging showed significant improvement in the diagnostic accuracy of PET-measured hyperemic MBF and MFR.

Keywords: Positron emission tomography; Computed tomography; Hybrid imaging; Lesion-specific myocardial blood flow; Coronary artery disease

INTRODUCTION

Myocardial perfusion positron emission tomography (PET) has the advantages of absolute quantification of myocardial blood flow (MBF) and flow reserve (MFR). It can measure volumetric flow normalized by a specific mass of myocardium without an invasive procedure. PET-measured MBF and MFR add diagnostic value to relative perfusion defect assessments[1)2)]

Journal of Cardiovascular Imaging JCVI

and facilitate the detection of multivessel disease causing balanced ischemia.[3] The prognostic value of PET-measured MFR for other traditional cardiovascular risk factors has been repeatedly demonstrated.[4-6]

Although the clinical values of MBF quantification using PET are evident, the lack of lesion-specificity limits its integration into the clinical management of coronary artery disease (CAD). PET-measured MBF does not always correlate well to a specific epicardial coronary stenosis due to the anatomical variability of the coronary trees.[7] Therefore, it is difficult to establish a normal MBF or MFR threshold or to determine revascularization based solely on MBF or MFR values.

Hybrid imaging of PET and coronary computed tomography (CT) has recently been suggested as an excellent candidate for the evaluation of CAD. The additional anatomical information provided by coronary CT enables correlation of perfusion abnormality with a specific epicardial coronary lesion[8] and a comprehensive interpretation of the relationship between CAD phenotypes and the changes of MBF.[9][10] Additional coronary CT images may help delineate the myocardium affected by a specific epicardial coronary lesion and evaluate the perfusion decrease in a lesion-specific manner. However, recent studies have failed to improve the diagnostic accuracy of PET-measured MBF parameters using hybrid PET/CT images.[8][11] They reassigned vascular territories in > 50% of the analyzed cases, but the reassignment did not lead to better diagnostic accuracy of hyperemic MBF. This might be attributed to the MBF quantification method used (vessel-specific MBF), which measures the MBF in a certain vascular territory as a whole, regardless of the lesion location.

Therefore, the present study assessed whether a more specific correlation of lesion location (proximal, mid, distal, or other small branches) using hybrid PET/CT imaging could improve the diagnostic accuracy of MBF parameters regarding anatomically significant left anterior descending artery (LAD) stenosis.

METHODS

Study population

Consecutive patients with stable angina referred to invasive coronary angiography (CAG) prospectively underwent N-13 ammonia PET and coronary CT before CAG for study purposes, all of which were performed within two weeks. The exclusion criteria included acute coronary syndrome, previous revascularization or myocardial infarction, overt heart failure with a decreased left ventricular ejection fraction (< 40%), changes in the clinical presentation between any two of the studies, a coronary anomaly, other structural heart diseases, or allergies to the contrast medium. Patients with a left main branch stenoses and those with data errors in the image fusion processes were also excluded. Forty-three patients were finally included and their baseline characteristics are listed in **Table 1**. The recruitment of the patients, acquisition and analysis of the imaging studies, and clinical data collection were approved by the Institutional Review Board (IRB) of Chonnam National University Hospital [IRB No. CNUH-2016-195].

N-13 ammonia PET

The N-13 ammonia PET was performed in accordance with the current guidelines for myocardial perfusion PET.[12] The patients fasted for ≥ 4 hours and nitrate, beta blockers,

https://doi.org/10.4250/jcvi.2019.0087

Journal of Cardiovascular Imaging JCVI

Table 1. Baseline characteristics of the study population

Characteristics	
Age (years)	63.0 ± 10.2
Males	30 (70)
Hypertension	20 (47)
Diabetes	16 (37)
Dyslipidemia	13 (30)
Body mass index (kg/m^2)	25.4 ± 3.8
Obesity (body mass index ≥ 25 kg/m^2)	19 (44)
Current smoker	3 (7)
Hemodynamics	
Resting heart rate (bpm)	66.5 ± 10.8
Resting systolic pressure (mmHg)	121.3 ± 9.3
Resting RPP (mmHg/min)	8,116.3 ± 1,196.0
Hyperemic heart rate (bpm)	82.9 ± 14.6
Hyperemic systolic pressure (mmHg)	112.6 ± 18.5
Hyperemic RPP (mmHg/min)	9,184.4 ± 25.0
Calcium score (total Agatston score)	341.9 ± 479.2

Data are the mean ± SD or n followed by percentage in parentheses.
CAD: coronary artery disease, RPP: rate-pressure product (systolic blood pressure × heart rate).

calcium channel blockers, methylxanthine derivatives, and caffeine were not consumed ≥ 24 hours before PET acquisition.

Patients were positioned on the scanner with their arms raised. Intravenous lines were placed in the patient's radial veins for N-13 ammonia injection and adenosine infusion. First, a low-dose CT scan (120 kV, 30 mA) for attenuation correction was performed. A bolus (11 MBq/kg [0.3 mCi/kg]) of N-13 ammonia was injected and the dynamic image acquisition was started simultaneously and lasted for six minutes. Immediately following the dynamic image acquisition, electrocardiogram (ECG)-gated static image acquisition was initiated and lasted 13 minutes. The infusion of adenosine was performed at a rate of 0.14 mg/kg/min for six minutes, one hour after the resting image acquisition was completed. N-13 ammonia was injected after three minutes during the peak hyperemia. Stress image acquisition was started simultaneously with the N-13 ammonia injection using the same time frames as the resting images. Image acquisition was performed using a dedicated PET scanner (Discovery ST, GE Healthcare, Chicago, IL, USA). The images were reconstructed using ordered subset expectation maximization with two iterations.

Coronary CT

One to two hours prior to the coronary CT scan, patients with a heart rate over 65 were administered p.o. beta blocker medication (propranolol 40 mg, maximum 120 mg).

A 2nd-generation dual-source CT scanner (SOMATOM Definition Flash; Siemens Medical Solution, Munich, Germany) was used while applying the previously described protocol.[10] The section thickness was 0.75 mm, the gantry rotation time was 0.33 s, the tube current was 600 mAs at 120 kVp, and the pitch was 0.2 (conventional mode) or 3.4 (high-pitch mode). ECG gating was performed either retrospectively (conventional mode) or prospectively (high-pitch or step-and-shoot mode), according to the patient's heart rate variability.

The CT scan range included the entire heart. A non-ionic contrast medium (Ultravist 370; Bayer Schering Pharma, Berlin, Germany) was injected as a bolus, followed by a 60 mL saline flush at a speed of 4 mL/s for clearance of the contrast medium. The axial images were reconstructed at multiple phases covering the cardiac cycle in increments of 10% of the RR

https://doi.org/10.4250/jcvi.2019.0087

interval between 5% and 95%. Short-axis slices were reconstructed from the base to the apex using the Argus software tool (Siemens Medical Solution).

Hybrid imaging of N-13 ammonia PET and coronary CT

The PET and CT images were fused using a commercially available software tool (CardIQ Fusion, GE Healthcare). The images were appropriately co-registered in the transaxial, coronal, and sagittal planes according to anatomical landmarks, such as the interventricular septum, cardiac apex, and papillary muscles. The epicardial surface was automatically extracted and manually modified using a seed and extend algorithm. The non-gated perfusion images were projected onto the myocardial surface using a rainbow color scale. The coronary trees were traced using the same algorithm as that used in the myocardial extraction. The perfusion-rendered myocardium and the extracted coronary trees were fused with the same axis orientation. The image fusion was performed using the Advantage Workstation 4.6 (GE Healthcare).

Conventional and lesion-specific MBF measurement

The analyses were performed only for the LAD as its path was invariably located along the anterior aspect of the interventricular septum with the least 'floating segments' among the three major coronary branches.

Conventional MBF measurements were performed using the PMOD (PMOD Technologies, Zurich, Switzerland) software package, as previously described.[10] The hyperemic and resting MBF was calculated for the standard 17 myocardial segments. The territory of the LAD included the apical, apical septal, apical anterior, mid-anterior, mid-anteroseptal, basal anterior, and basal anteroseptal segments.[13] The MFR was calculated by dividing the hyperemic MBF with the correlating resting MBF.

Two cardiac imaging experts analyzed the coronary CT images to assess the presence and location of LAD stenosis. Any stenosis (≥ 30%)[14] on the CT images was considered eligible for lesion-specific MBF measurement and its location was classified as proximal, mid-, distal LAD, and diagonal branches, as previously suggested.[15] The hybrid PET/CT images were aligned to the same axis as that of the polar plot MBF maps from the PMOD software. According to the vascular path and the location of a certain stenosis, the downstream myocardial segments were isolated by the consensus of two observers. The lesion-specific MBF was defined as the average MBF value calculated within the isolated myocardial segments (**Figure 1**).

Radiation exposure from hybrid PET/CT imaging

The total radiation exposure of a patient undergoing hybrid PET/CT imaging was calculated by summing the effective doses from the N-13 ammonia PET and coronary CT studies, respectively. The effective dose from N-13 ammonia PET was calculated by multiplying the estimated effective dose (0.002 mSv/MBq) suggested by the International Commission on Radiological Protection Publication 80[16] with the actual administered dose (produced N-13 activity – post-injection activity in the syringe). The effective doses from rest and stress studies were summed to obtain the total radiation exposure from N-13 ammonia PET. For calculating the effective dose from coronary CT, the dose-length product was obtained from the CT dose report and multiplied by a conversion coefficient value of 0.014 $mSv \cdot mGy^{-1}cm^{-1}$.[17] The effective dose from the low-dose attenuation correction CT was calculated using the same method as that of cardiac CT with a conversion coefficient value of

https://doi.org/10.4250/jcvi.2019.0087

Journal of Cardiovascular Imaging JCVI

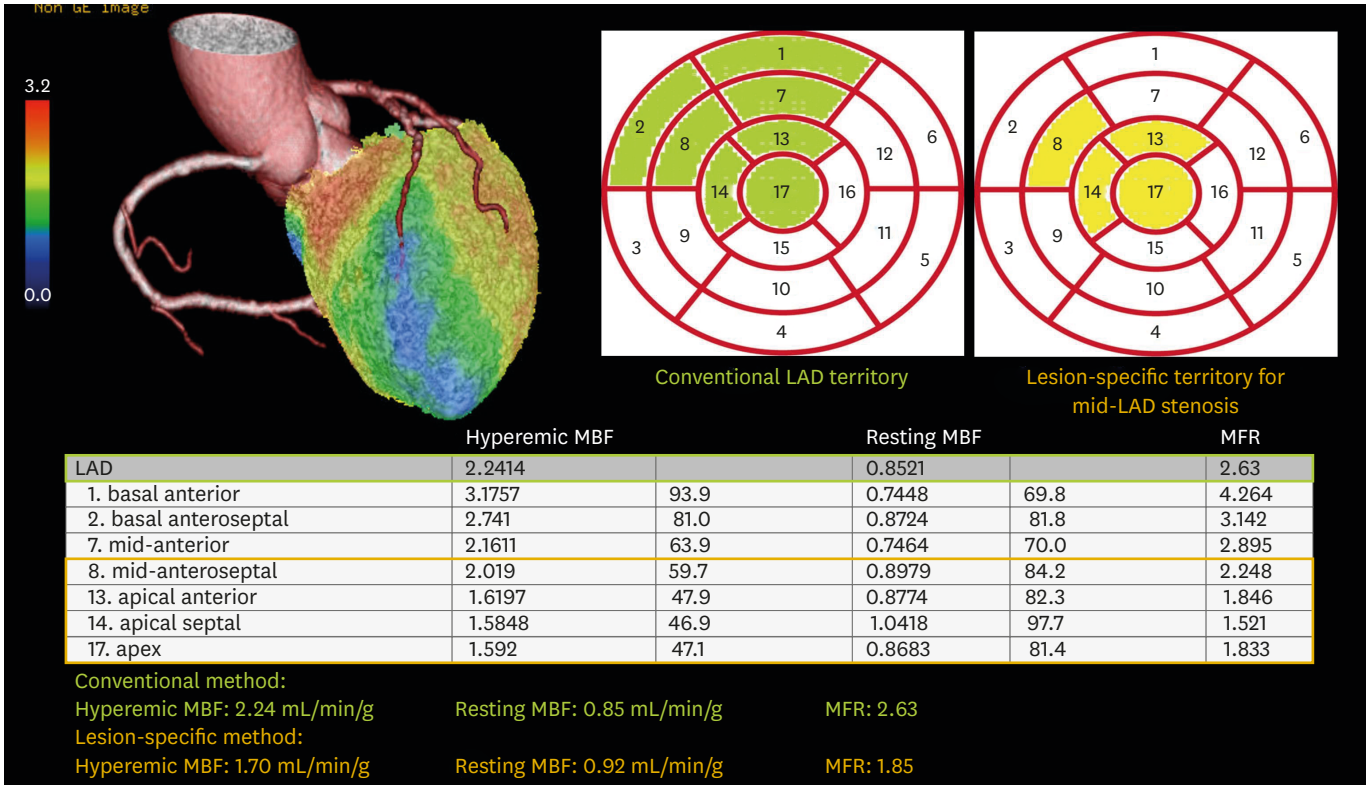

	Hyperemic MBF		Resting MBF		MFR
LAD	2.2414		0.8521		2.63
1. basal anterior	3.1757	93.9	0.7448	69.8	4.264
2. basal anteroseptal	2.741	81.0	0.8724	81.8	3.142
7. mid-anterior	2.1611	63.9	0.7464	70.0	2.895
8. mid-anteroseptal	2.019	59.7	0.8979	84.2	2.248
13. apical anterior	1.6197	47.9	0.8774	82.3	1.846
14. apical septal	1.5848	46.9	1.0418	97.7	1.521
17. apex	1.592	47.1	0.8683	81.4	1.833

Conventional method:
Hyperemic MBF: 2.24 mL/min/g Resting MBF: 0.85 mL/min/g MFR: 2.63
Lesion-specific method:
Hyperemic MBF: 1.70 mL/min/g Resting MBF: 0.92 mL/min/g MFR: 1.85

Figure 1. Conventional and lesion-specific measurements of the MBF and MFR in a patient with a significant mid-LAD stenosis (89% reference diameter). For a lesion-specific MBF measurement, the segments downstream of the mid-LAD stenosis (segments 8, 13, 14, and 17) were isolated and their average MBF values were obtained. LAD: left anterior descending artery, MBF: myocardial blood flow, MFR: myocardial flow reserve.

0.014 $mSv \cdot mGy^{-1}cm^{-1}$.[18] This value was regarded to be a part of the effective dose from N-13 ammonia PET.

Statistical analyses

The hyperemic MBF, resting MBF, and MFR values were compared between the LADs with and without significant stenosis (≥ 70% reference diameter on CAG)[19] using the student's t-test. To evaluate the changes of the MBF values by applying the lesion-specific method, the MBF values measured by the two different methods were compared using the paired t-test.

The diagnostic performances were compared between conventional and lesion-specific measurements. The sensitivity, specificity, negative predictive value (NPV), positive predictive value (PPV), and accuracy with 95% confidence intervals were calculated for the two methods, based on the binary discrimination of either the presence or absence of significant stenosis. Receiver operating characteristics (ROC) curve analysis was performed to obtain the optimal cutoff values for the calculation of diagnostic performances. The areas under the ROC curves (accuracy) were compared using the methodology suggested by DeLong *et al.*[20] Pearson's correlation analysis was applied to elucidate the relationships between the MBF values measured by the two different methods and anatomical stenosis severity.

The statistical analyses were performed using IBM SPSS Statistics for Windows, ver. 23.0 (IBM Corp., Armonk, NY, USA) and MedCalc ver. 11.6.1.0 (MedCalc Software bvba, USA). A p-value < 0.05 was considered as statistically significant.

https://doi.org/10.4250/jcvi.2019.0087

Journal of Cardiovascular Imaging JCVI

RESULTS

Twenty-eight patients (64%) were eligible for lesion-specific MBF measurement and the measurements were successfully performed for all of them. Nineteen (44%) had significant LAD stenoses. The significant stenoses were located in the proximal LAD (n = 5), mid-LAD (n = 10), proximal-to-mid-LAD (n = 3), and the diagonal branch (n = 1). No patients had significant stenosis in the distal LAD. The myocardial segments downstream of the proximal lesion were included for lesion-specific MBF measurement in those with proximal to mid-LAD stenoses.

The hyperemic MBF and MFR measured using the lesion-specific method were significantly lower than those measured using the conventional method while the resting MBF was similar between the two methods (**Figure 2**). The hyperemic MBF and MFR were significantly lower in the LADs with significant stenosis for both the conventional and lesion-specific measurements, while no difference of the resting MBF was found (**Figure 3**).

For the conventional method, the sensitivity, specificity, NPV, PPV, and accuracy were 71%, 68%, 74%, 65%, and 70% for the hyperemic MBF (optimal cutoff = 2.15 mL/min/g) and 79%, 63%, 74%, 65%, and 70% for the MFR (optimal cutoff = 1.82), respectively. For the lesion-specific method, the sensitivity, specificity, NPV, PPV, and accuracy were 83%, 74%, 80%, 78%, and 80% for the hyperemic MBF (optimal cutoff = 1.75 mL/min/g) and 79%, 79%, 83%, 75%, and 79% for the MFR (optimal cutoff = 1.86), respectively. The overall diagnostic accuracy was significantly higher with the lesion-specific method for both the hyperemic MBF and MFR. However, no statistical differences were found between the diagnostic accuracy of the hyperemic MBF and MFR when the same method was applied (**Figure 4**). The resting MBF could not effectively detect significant LAD stenosis using either of the two methods. The hyperemic MBF and MFR measured by the lesion-specific method correlated better with anatomical stenosis severity than those measured by the conventional method (**Figure 5**).

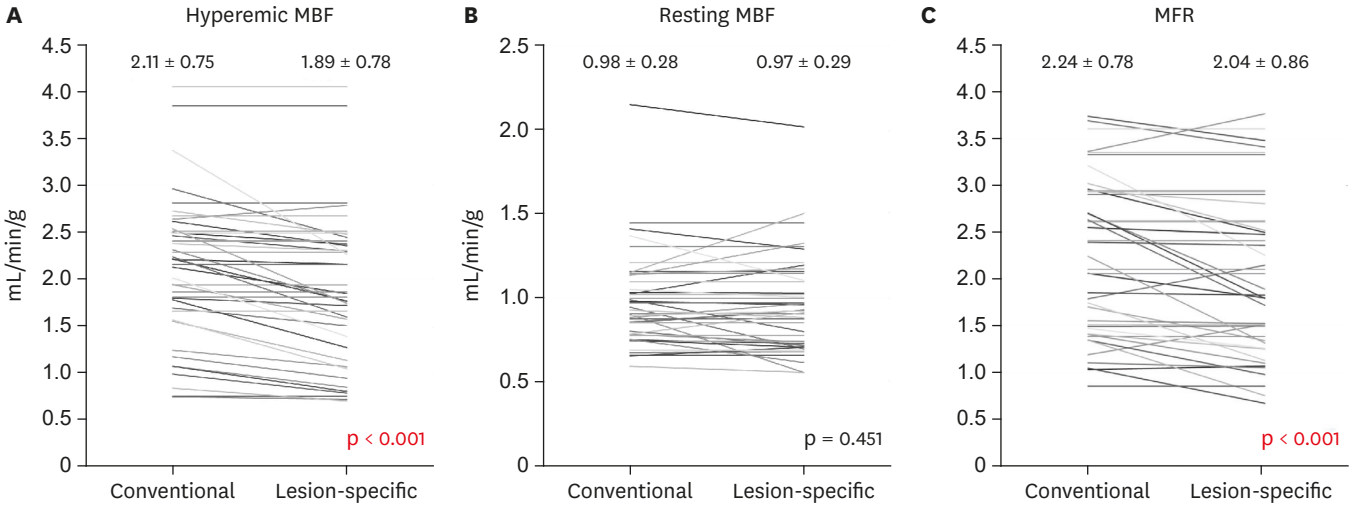

Figure 2. Comparison of MBF and MFR measured by conventional and lesion-specific methods.
The hyperemic MBF and MFR significantly decreased after applying lesion-specific measurement, while the resting MBF remained similar. MBF: myocardial blood flow, MFR: myocardial flow reserve.

https://doi.org/10.4250/jcvi.2019.0087

Journal of Cardiovascular Imaging JCVI

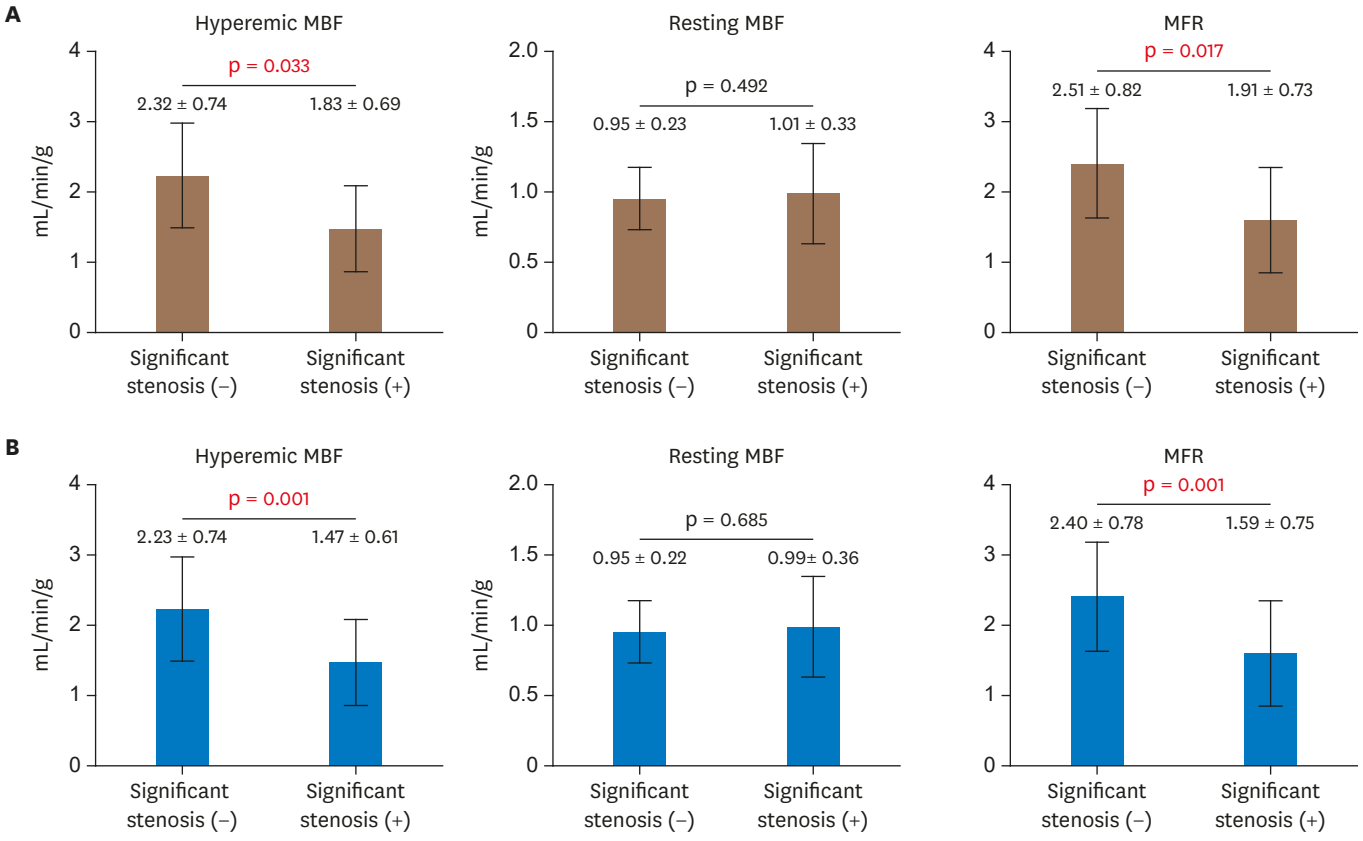

Figure 3. Comparison of the MBF and MFR between LADs with and without significant stenosis for conventional (A) and lesion-specific (B) methods. LAD: left anterior descending artery, MBF: myocardial blood flow, MFR: myocardial flow reserve.

The mean effective dose from hybrid PET/CT imaging was 9.15 ± 5.48 mSv. The mean effective dose from N-13 ammonia PET was 1.94 ± 0.12 mSv while that from cardiac CT was 7.21 ± 5.45 mSv. However, the highest effective dose reached 20.9 mSv in a patient imaged in the conventional mode.

DISCUSSION

The present study assessed MBF measurements using hybrid PET/CT imaging. The lesion-specific method significantly improved the diagnostic accuracy of PET-measured MBF parameters compared to the conventional method. The lesion-specific hyperemic MBF and MFR were better correlated with the anatomical severity of LAD stenosis than conventional methods.

The anatomy of the coronary trees varied among individuals and the 17 segment model has substantial discrepancies with actual coronary territories.[21] These facts seriously limit the clinical relevance of MBF parameters derived from myocardial perfusion PET. Two recent studies attempted to solve these problems by reassigning vascular territories using hybrid PET/CT.[8][11] However, although 50% of the standard myocardial segments were reassigned to new territories, they failed to improve the diagnostic accuracy of the hyperemic MBF regarding anatomically and functionally significant stenoses. In those studies, the hyperemic MBF values were averaged throughout the whole territory, regardless of the lesion locations so that only small changes were observed after territory reassignment. In contrast, the

https://doi.org/10.4250/jcvi.2019.0087

Journal of Cardiovascular Imaging JCVI

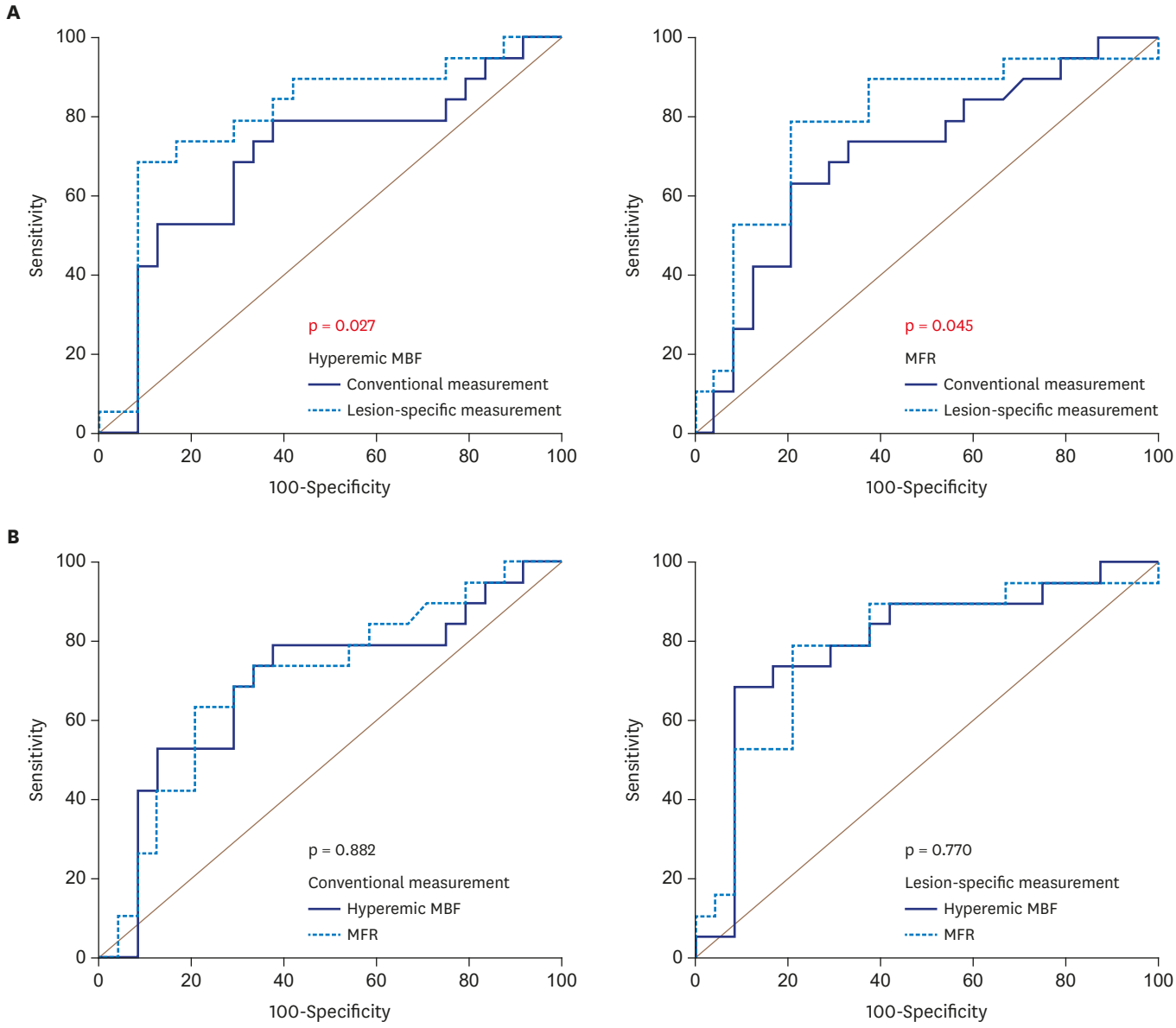

Figure 4. Comparison of the diagnostic accuracy according to the measurement method (A) and MBF parameters (B). MBF: myocardial blood flow, MFR: myocardial flow reserve.

hyperemic MBF and MFR values could significantly decrease if the lesion locations were taken into account, as shown in the present study. It can be assumed that a whole territory-based, 'per-vessel' approach may dilute the significance of coronary stenosis. Some normally perfused segments, which are not subtended to the stenosis, might falsely increase the hyperemic MBF and lower its diagnostic performance. The MBF parameters calculated only within the downstream segments could more directly reflect the severity of myocardial ischemia.

There have been several attempts to measure MBF in a lesion-specific manner using hybrid PET/CT imaging. Kim *et al.*[22] traced the MBF change by manually drawing ellipsoidal regions of interest along the interventricular septum on PET images. The results showed that the MBF gradient reflected the location (proximal vs. mid-to-distal) of the LAD stenosis. Piccinelli *et al.*[23] introduced a more advanced technique of tracking the vascular path and its

https://doi.org/10.4250/jcvi.2019.0087

Journal of Cardiovascular Imaging JCVI

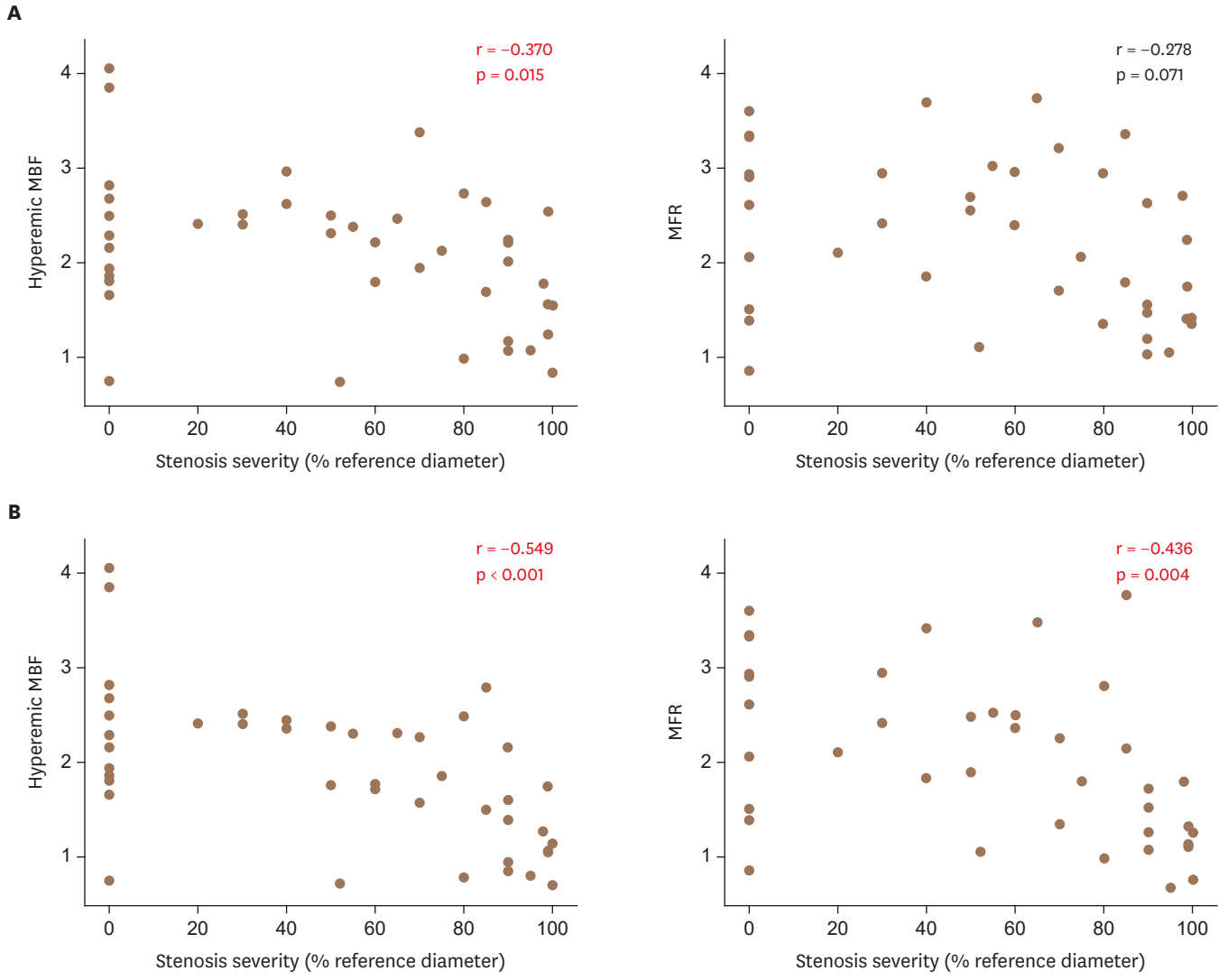

Figure 5. Correlation between the MBF parameters and anatomical stenosis severity for conventional (A) and lesion-specific (B) methods. MBF: myocardial blood flow, MFR: myocardial flow reserve.

MBF changes along the coronary arteries. They established normal ranges for vessel-specific MBF values from subjects without angiographic stenoses. Without additional anatomical information from CT, Lee *et al.*[2] analyzed only the segments with visually appreciable perfusion defects to enhance the lesion specificity of the MBF parameters. The main limitation of such a method is that visual estimation of the extent of perfusion defects can be influenced by threshold and image contrasts. Notably, recent coronary CT studies have suggested automated delineation of individualized coronary territories named fractional myocardial mass (FMM), which is completely independent of the standardized 17 myocardial segment model.[24][25] A larger FMM relative to the coronary luminal area was associated with lower fractional flow reserve (FFR) values,[26] which is plausible since FFR reflects not only the severity of epicardial coronary stenosis but also the myocardial mass subtended to a specific coronary segment. Taking advantage of hybrid PET/CT imaging, the amount of actual flow normalized to the subtended myocardium ('FMM-specific MBF') may be available, providing comprehensive insight into the coronary physiology among the pressure, flow, and myocardial mass.

https://doi.org/10.4250/jcvi.2019.0087

There are concerns that hybrid PET/CT imaging may be redundant in the non-invasive assessment of CAD and that coronary CT itself may be sufficient. As FFR measured by CT has become clinically available, coronary CT has gained relevance in both the anatomical and functional assessments of epicardial CAD.[27] However, a patient's prognosis depends not only on the severity of epicardial stenosis, but also on hemodynamic impairments caused by diffuse atherosclerosis or microvascular disease. FFR may overlook significant epicardial stenosis in the presence of microvascular dysfunction, which blunts the vasodilatory response to pharmacologic stress.[28] Therefore, there is still a great need for measuring flow that can be obtained by PET. Myocardial perfusion PET and coronary CT can play complementary roles through their respective genuine abilities, leading to synergistic and comprehensive evaluations of various aspects of CAD.

There are several limitations of the present study. First, the sample size was small and the physiological stenosis severity (such as FFR) was not assessed. Second, actual clinical application of the lesion-specific MBF measurement may be limited in the case of the left main stem, left circumflex, or right coronary artery stenoses because they have substantial floating segments, which do not directly correlate with certain myocardial areas. Third, we did not optimize the coronary CT protocol in order to reduce radiation exposure in this hybrid imaging study. Although the mean total effective dose was under 10 mSv, which is comparable to recent data[29] and similar to or lower than that from SPECT using Tc-99m-labeled agents and conventional cameras,[30] the highest value obtained was > 20 mSv. This implies that the coronary CT protocol should be optimized for the balance between the diagnostic gain from hybrid imaging and radiation risk. Lastly, albeit significantly improved, the diagnostic accuracy of lesion-specific hyperemic MBF and MFR was slightly lower than that of the vessel-specific hyperemic MBF assessed in recent studies.[8][11] Regarding the fact that the prevalence of diabetes was more than double in our study (37% vs. 16%), underlying microvascular disease might have negatively influenced the diagnostic accuracy regarding epicardial stenosis. Additionally, the calcium scores were substantially high in our study population, which might have decreased the MFR even in the absence of significant epicardial stenosis.[10]

Conclusions

Lesion-specific measurement using hybrid imaging of myocardial perfusion PET and coronary CT improved the diagnostic accuracy of PET-measured hyperemic MBF and MFR. This technique may overcome the shortcomings of the current MBF measurement by PET and help to diagnose and manage CAD in the clinical field.

ACKNOWLEDGMENTS

This work was supported by a grant (NRF-2016R1D1A3B01006631) of the Basic Science Research Program through the National Research Foundation (NRF) funded by the Ministry of Education, Republic of Korea.

REFERENCES

1. Fiechter M, Ghadri JR, Gebhard C, et al. Diagnostic value of 13N-ammonia myocardial perfusion PET: added value of myocardial flow reserve. *J Nucl Med* 2012;53:1230-4.
PUBMED | CROSSREF

2. Lee JM, Kim CH, Koo BK, et al. Integrated myocardial perfusion imaging diagnostics improve detection of functionally significant coronary artery stenosis by 13N-ammonia positron emission tomography. *Circ Cardiovasc Imaging* 2016;9:e004768.
PUBMED | CROSSREF

3. Ziadi MC, Dekemp RA, Williams K, et al. Does quantification of myocardial flow reserve using rubidium-82 positron emission tomography facilitate detection of multivessel coronary artery disease? *J Nucl Cardiol* 2012;19:670-80.
PUBMED | CROSSREF

4. Herzog BA, Husmann L, Valenta I, et al. Long-term prognostic value of 13N-ammonia myocardial perfusion positron emission tomography added value of coronary flow reserve. *J Am Coll Cardiol* 2009;54:150-6.
PUBMED | CROSSREF

5. Taqueti VR, Hachamovitch R, Murthy VL, et al. Global coronary flow reserve is associated with adverse cardiovascular events independently of luminal angiographic severity and modifies the effect of early revascularization. *Circulation* 2015;131:19-27.
PUBMED | CROSSREF

6. Gupta A, Taqueti VR, van de Hoef TP, et al. Integrated noninvasive physiological assessment of coronary circulatory function and impact on cardiovascular mortality in patients with stable coronary artery disease. *Circulation* 2017;136:2325-36.
PUBMED | CROSSREF

7. Cho SG, Kim HS, Bom HH. Flow-based functional assessment of coronary artery disease by myocardial perfusion positron emission tomography in the era of fractional flow reserve. *Ann Nucl Cardiol* 2016;2:99-105.
CROSSREF

8. Thomassen A, Petersen H, Johansen A, et al. Quantitative myocardial perfusion by O-15-water PET: individualized vs. standardized vascular territories. *Eur Heart J Cardiovasc Imaging* 2015;16:970-6.
PUBMED | CROSSREF

9. Dey D, Diaz Zamudio M, Schuhbaeck A, et al. Relationship between quantitative adverse plaque features from coronary computed tomography angiography and downstream impaired myocardial flow reserve by 13N-ammonia positron emission tomography: a pilot study. *Circ Cardiovasc Imaging* 2015;8:e003255.
PUBMED | CROSSREF

10. Cho SG, Park KS, Kim J, et al. Coronary flow reserve and relative flow reserve measured by N-13 ammonia PET for characterization of coronary artery disease. *Ann Nucl Med* 2017;31:144-52.
PUBMED | CROSSREF

11. Bom MJ, Schumacher SP, Driessen RS, et al. Impact of individualized segmentation on diagnostic performance of quantitative positron emission tomography for haemodynamically significant coronary artery disease. *Eur Heart J Cardiovasc Imaging* 2019;20:525-32.
PUBMED | CROSSREF

12. Dilsizian V, Bacharach SL, Beanlands RS, et al. ASNC imaging guidelines/SNMMI procedure standard for positron emission tomography (PET) nuclear cardiology procedures. *J Nucl Cardiol* 2016;23:1187-226.
PUBMED | CROSSREF

13. Cerqueira MD, Weissman NJ, Dilsizian V, et al.. Standardized myocardial segmentation and nomenclature for tomographic imaging of the heart. A statement for healthcare professionals from the Cardiac Imaging Committee of the Council on Clinical Cardiology of the American Heart Association. *Int J Cardiovasc Imaging* 2002;18:539-42.
PUBMED

14. Nørgaard BL, Terkelsen CJ, Mathiassen ON, et al. Coronary CT angiographic and flow reserve-guided management of patients with stable ischemic heart disease. *J Am Coll Cardiol* 2018;72:2123-34.
PUBMED | CROSSREF

15. George RT, Arbab-Zadeh A, Cerci RJ, et al. Diagnostic performance of combined noninvasive coronary angiography and myocardial perfusion imaging using 320-MDCT: the CT angiography and perfusion methods of the CORE320 multicenter multinational diagnostic study. *AJR Am J Roentgenol* 2011;197:829-37.
PUBMED | CROSSREF

16. ICRP. ICRP publication 80: Radiation dose to patients from radiopharmaceuticals (addendum 2 to ICRP publication 53). *Ann ICRP* 1998;28:1-126.

17. Trattner S, Halliburton S, Thompson CM, et al. Cardiac-specific conversion factors to estimate radiation effective dose from dose-length product in computed tomography. *JACC Cardiovasc Imaging* 2018;11:64-74.
PUBMED | CROSSREF

18. Christner JA, Kofler JM, McCollough CH. Estimating effective dose for CT using dose-length product compared with using organ doses: consequences of adopting International Commission on Radiological Protection publication 103 or dual-energy scanning. *AJR Am J Roentgenol* 2010;194:881-9.
PUBMED | CROSSREF

19. Maddox TM, Stanislawski MA, Grunwald GK, et al. Nonobstructive coronary artery disease and risk of myocardial infarction. *JAMA* 2014;312:1754-63.
PUBMED | CROSSREF

20. DeLong ER, DeLong DM, Clarke-Pearson DL. Comparing the areas under two or more correlated receiver operating characteristic curves: a nonparametric approach. *Biometrics* 1988;44:837-45.
PUBMED | CROSSREF

21. Donato P, Coelho P, Santos C, Bernardes A, Caseiro-Alves F. Correspondence between left ventricular 17 myocardial segments and coronary anatomy obtained by multi-detector computed tomography: an ex vivo contribution. *Surg Radiol Anat* 2012;34:805-10.
PUBMED | CROSSREF

22. Kim HS, Cho SG, Kim JH, Bom HS. Indirect radionuclide coronary angiography to evaluate gradients of myocardial blood flow and flow reserve through coronary stenosis using N-13 ammonia PET/CT. *Chonnam Med J* 2013;49:69-74.
PUBMED | CROSSREF

23. Piccinelli M, Cho SG, Garcia EV, et al. Vessel-specific quantification of absolute myocardial blood flow, myocardial flow reserve and relative flow reserve by means of fused dynamic $^{13}NH_3$ PET and CCTA: ranges in a low-risk population and abnormality criteria. *J Nucl Cardiol* 2018 Oct 29 E-pub ahead of print, https://doi.org/10.1007/s12350-018-01472-3.
PUBMED | CROSSREF

24. Kim HY, Lim HS, Doh JH, et al. Physiological severity of coronary artery stenosis depends on the amount of myocardial mass subtended by the coronary artery. *JACC Cardiovasc Interv* 2016;9:1548-60.
PUBMED | CROSSREF

25. Kim HY, Doh JH, Lim HS, et al. Identification of coronary artery side branch supplying myocardial mass that may benefit from revascularization. *JACC Cardiovasc Interv* 2017;10:571-81.
PUBMED | CROSSREF

26. Yang DH, Kang SJ, Koo HJ, et al. Incremental value of subtended myocardial mass for identifying FFR-verified ischemia using quantitative CT angiography: comparison with quantitative coronary angiography and CT-FFR. *JACC Cardiovasc Imaging* 2019;12:707-17.
PUBMED | CROSSREF

27. Gaur S, Øvrehus KA, Dey D, et al. Coronary plaque quantification and fractional flow reserve by coronary computed tomography angiography identify ischaemia-causing lesions. *Eur Heart J* 2016;37:1220-7.
PUBMED | CROSSREF

28. van de Hoef TP, Siebes M, Spaan JA, Piek JJ. Fundamentals in clinical coronary physiology: why coronary flow is more important than coronary pressure. *Eur Heart J* 2015;36:3312-9a.
PUBMED | CROSSREF

29. Kajander S, Ukkonen H, Sipilä H, Teräs M, Knuuti J. Low radiation dose imaging of myocardial perfusion and coronary angiography with a hybrid PET/CT scanner. *Clin Physiol Funct Imaging* 2009;29:81-8.
PUBMED | CROSSREF

30. Einstein AJ. Effects of radiation exposure from cardiac imaging: how good are the data? *J Am Coll Cardiol* 2012;59:553-65.
PUBMED | CROSSREF